Transition from ballistic to diffusive heat transfer in a chain with breaks

Anton M. Krivtsov ⬤, Vitaly A. Kuzkin ⬤, and Vadim A. Tsaplin ⬤

Peter the Great Saint Petersburg Polytechnic University, Saint Petersburg 195251, Russia
and Institute for Problems in Mechanical Engineering RAS, Saint Petersburg 199178, Russia

The transition from a ballistic to a diffusive regime of heat transfer is studied using two models. The first model is a one-dimensional chain with bonds, capable of dissociation. Interparticle forces in the chain are harmonic for bond deformations below a critical value, corresponding to the dissociation, and zero above this value. A kinetic description of heat transfer in the chain is proposed using the second model, namely, a gas of noninteracting quasiparticles, reflecting from randomly occurring barriers. The motion of quasiparticles mimics heat (energy) transfer in the chain, while the barriers mimic dissociated bonds. For the gas, a kinetic equation is derived and solved analytically. The solution demonstrates the transition from the ballistic regime at small times to the diffusive regime at large times. In the diffusive limit, the distance traveled by a heat obeys square-root asymptotics as in the case of classical diffusion. However, the shape of the fundamental solution for temperature differs from the Gaussian function and therefore the Fourier law is not satisfied. Two examples are considered to demonstrate that the presented kinetic model is in good qualitative agreement with the results of the numerical solution of the chain dynamics. The presented results show that bond dissociation is an important mechanism underlying the transition from ballistic to diffusive heat transfer in one-dimensional chains.

I. INTRODUCTION

At macroscopic spatial and temporal scales, the heat transfer is usually diffusive and well described by the Fourier law. Experiments of the last decades show that at micro- and nanoscale, significant deviations from the Fourier law are observed (see, e.g., reviews [1,2]). In particular, in materials with low defect density the heat propagates in a wavelike manner and the so-called ballistic heat transfer regime is realized [3–6]. Therefore heat transfer regimes at small and large scales are different, and an understanding of the physical mechanisms underlying the transition between these regimes is of great fundamental and practical importance.

In literature, one-dimensional chains are often used for the investigation of different heat transfer regimes (see, e.g., reviews [7–9]). In harmonic chains, the heat transfer is purely ballistic [10–12]. Adding anharmonicity allows one to consider both quasiballistic (at small spatial and temporal scales [13–16]) and diffusive [9] heat transfer. However, in the majority of one-dimensional systems the diffusion of heat is anomalous: the Fourier law is not satisfied and the effective thermal conductivity diverges with increasing system size [9]. In papers [17,18], it is shown numerically that convergence of the thermal conductivity is achieved in chains with bonds capable of dissociation. Bond dissociation, caused by thermal motion, leads to reflection of elastic waves carrying energy. Multiple reflections results in a transition from a ballistic to a diffusive regime of heat transfer. The present paper focuses on an analytical description of this transition.

Different regimes of heat transfer can be described, for example, in the framework of kinetic theory [19]. In the kinetic theory, the heat transfer is modeled by the motion of the so-called quasiparticles, carrying energy. The key quantity of the kinetic theory is the distribution function, describing the distribution of a quasiparticle's coordinates and velocities. Evolution of the distribution function is governed by the Boltzmann equation. For harmonic and weakly anharmonic chains the relation between lattice dynamics and kinetic models of heat transfer can be obtained rigorously. In particular, harmonic chains are considered, for example, in papers [20,21], while weakly anharmonic chains are considered in papers [20,22,23]. However, these papers are limited to the β-FPUT (Fermi-Pasta-Ulam-Tsingou) model without bond dissociation. To the best of our knowledge, derivation of kinetic equations from lattice dynamics for chains with bond dissociation is not presented in the literature. However, in some cases the heat transfer is described using heuristic assumptions about the motion of quasiparticles. In particular, in papers [24–26] it is shown that anomalous heat transfer can be described by assuming that the quasiparticles perform the Levy walk. In the present paper, we use a similar heuristic approach. The simplest chain with bond dissociation, further refered to as the chain with breaks, is considered. In this chain, the interparticle force is harmonic for deformations of the bonds below a critical value, corresponding to bond dissociation, and zero above this value. This model allows one to ignore the interaction of quasiparticles, caused by "smooth nonlinearity," and to assume that the quasiparticles are reflected from the dissociated bonds and move freely between the reflections.

The main goal of the present paper is an analytical description of heat transfer in the chain with breaks in the framework of kinetic theory. Unsteady heat transport, i.e., the evolution of the initial temperature profile (or initial heat flux) is considered. The transition from a ballistic to a non-Fourier diffusive regime is demonstrated and analyzed.

The paper is organized as follows. In Sec. II, equations of motion for the chain with breaks and initial conditions, corresponding to the initial temperature profile, are formulated. The probability of bond dissociation at different temperatures is calculated. In Sec. III, a kinetic equation describing the heat transfer is derived and solved. In Sec. IV, two functions allowing one to distinguish different regimes of heat transfer are introduced. Ballistic and diffusive regimes and the transition between them are investigated. In Sec. V, the relation between properties of the fundamental solution and length dependence of the effective thermal conductivity is discussed. It is demonstrated, in particular, that finite thermal conductivity, in general, is not necessarily equivalent to fulfillment of the Fourier law. In Sec. VI, decay of a sinusoidal temperature profile is studied analytically and numerically at different densities of bond breaks. In Sec. VII, the decay of the initially excited heat flux in the chain with uniform temperature profile is investigated. The relation between lattice dynamics and kinetic theory is discussed in Sec. VIII.

II. CHAIN WITH BREAKS

A. Statement of the heat transport problem

We consider a one-dimensional chain consisting of particles interacting with the nearest neighbors. The interparticle force is linear until the bond deformation reaches some critical value, corresponding to the dissociation. For bond deformations above the critical value, the force is equal to zero. Dynamics of the crystal is described by equations of motion

$$m\ddot{u}_n = F_{n+1} - F_n,$$
$$F_n = C(u_n - u_{n-1})\theta(a\varepsilon_* - u_n + u_{n-1}), \quad (1)$$

where m is the particle mass, u_n is the displacement of the particle n, θ is the Heaviside step function,[1] C is the bond stiffness, a is the equilibrium bond length, and ε_* is the critical strain corresponding to bond dissociation. Further, it is shown that bond dissociation, caused by the thermal motion, leads to the reflection of waves carrying energy and the transition from a ballistic to a diffusive (non-Fourier) regime of heat transfer.

The model (1) can be considered as the simplest modification of the harmonic crystal, which allows one to consider the influence of bond dissociation and to exclude all other anharmonic effects, influencing the heat transfer in more complicated models of Lennard-Jones type. In the case $\varepsilon_* = 0$, it coincides with the elastic rod model, numerically studied in paper [17]. We note that the case $\varepsilon_* = 0$ corresponds to poorly repulsive interactions between the particles.

Since the interparticle force (1) vanishes for bond strains exceeding ε_*, each dissociated bond separates the chain into two noninteracting fragments. If the chain is subjected to free boundary conditions, then these fragments after the separation may not meet again. To prevent this irreversible fragmentation, we fix the total length of the chain $L = Na$ using the periodic boundary conditions

$$u_{n+N} \equiv u_n, \quad (2)$$

where N is the number of particles in the periodic cell.

In the absence of breaks ($\varepsilon_* = \infty$), interactions between the particles are linear and Eq. (1) describes the dynamics of the so-called Hooke chain [27]:

$$m\ddot{u}_n = C(u_{n+1} - 2u_n + u_{n-1}). \quad (3)$$

The dispersion relation $\omega(\kappa)$ and the group velocity $c_g(\kappa)$ for the Hooke chain are given by

$$\omega^2(\kappa) = \frac{4C}{m}\sin^2(\pi\kappa), \quad c_g(\kappa) = c\cos(\pi\kappa), \quad (4)$$

where $\kappa \in [0; 1]$, $c = a\sqrt{C/m}$ is the sound speed.

The initial temperature profile and zero heat fluxes are created in the system using the following stochastic initial conditions (nonzero flux is considered in Sec. VII):

$$u_n = 0, \quad \dot{u}_n = \varrho_n\sqrt{\frac{2k_B}{m}T_0(na)}, \quad \langle\varrho_n\rangle = 0,$$
$$\langle\varrho_n\varrho_p\rangle = \delta_{np}, \quad (5)$$

where $T_0(na)$ is the desired kinetic temperature profile (6) [limitations on the function $T_0(x)$ are discussed below; see formula (8)], ϱ_n are uncorrelated random numbers with zero mean and unit variance, δ_{np} is the Kroneker delta, and brackets $\langle\cdots\rangle$ stand for mathematical expectation. The multiplier $\sqrt{2}$ in the expression for initial velocities is introduced in order to compensate the decrease of temperature due to the transition of nearly a half of the kinetic energy into the potential energy (discussion of this transition is presented, e.g., in papers [11,28]). The initial conditions (5) can be considered, for example, as a result of heating by an ultrashort laser pulse.

To introduce the kinetic temperature, the infinite number of realizations of the system (1) with random initial conditions (5) is considered. The kinetic temperature $T(na)$ of the particle n is defined as

$$k_B T(na) = m\langle\dot{u}_n^2\rangle, \quad (6)$$

where k_B is the Boltzmann constant. In numerical modeling, the mathematical expectation in (6) is approximately replaced by the average over a large number of realizations:

$$k_B T(na) \approx m\langle\dot{u}_n^2\rangle_r = \frac{m}{N_r}\sum_{i=1}^{N_r}\left(\dot{u}_n^{(i)}\right)^2, \quad (7)$$

where $\dot{u}_n^{(i)}$ is the velocity of particle n in the realization number i and N_r is the total number of realizations.

Further, we study the evolution of the temperature profile in the chain and propose a kinetic model of this process.

B. Temperature dependence of density of breaks

The key quantity of the considered model is the density of breaks q, defined as the mathematical expectation of the number of dissociated bonds per unit length. This parameter enters the kinetic model of heat transfer, developed in Sec. III. In the present subsection, we find the relation between q and the parameters of the initial value problem for the chain (1), (5).

The density of breaks depends on temperature and therefore it may change during the heat transfer process. To

---

[1]By the definition $\theta(x) = 0$ for $x < 0$ and $\theta(x) = 1$ for $x \geqslant 0$.

minimize the influence of changes in temperature on the density of breaks, we consider functions $T_0(x)$ such that

$$T_0(x) = T_b + \Delta T(x), \quad \max|\Delta T(x)| \ll T_b, \quad (8)$$

where T_b is the background temperature.

The question arises as to how small the ratio $\max|\Delta T(x)|/T_b$ should be such that the influence of the nonuniform distribution of temperature on the density of breaks and on heat transfer can be neglected. To answer this question, we calculate the density of breaks q corresponding to temperature T_b. We use the following expression for the strain distribution function $\zeta(\varepsilon)$[2] (see the Appendix for derivation):

$$\zeta(\varepsilon) = \zeta_0 \, \exp\left(-\frac{Ca^2\min(\varepsilon, \varepsilon_*)^2 + 2p_T a\varepsilon}{2k_B T_b}\right), \quad (9)$$

where p_T is the thermal pressure, equal to the negative average force acting between two neighboring particles. To find the unknown ζ_0 and p_T in formula (9), we use the normalization condition for the distribution function ζ and the fact that the average strain under periodic boundary conditions is equal to zero:

$$\int_{-\infty}^{+\infty} \zeta(\varepsilon)d\varepsilon = 1, \quad \int_{-\infty}^{+\infty} \varepsilon\zeta(\varepsilon)d\varepsilon = 0. \quad (10)$$

Substituting (9) into (10) yields the system of equations with respect to ζ_0 and p_T. The first equation in (10) relates ζ_0 and p_T, while the second equation serves for calculation of p_T.

Given the known strain distribution function $\zeta(\varepsilon)$, the density of breaks is calculated as

$$qa = \int_{\varepsilon_*}^{+\infty} \zeta(\varepsilon)d\varepsilon, \quad (11)$$

where the right-hand side is the probability that the strain exceeds ε_*. Using (9)– (11) we derive the following relation between the density of breaks, T_b and p_T:

$$qa = \frac{p_T^2}{C(p_T a\varepsilon_* + k_B T_b)}. \quad (12)$$

The thermal pressure is calculated by substituting (9) into the second equation from (10). The substitution yields a transcendental equation with respect to p_T, which can be solved numerically.

At low temperatures ($T_b \to 0$), the density of breaks q and the thermal pressure p_T are represented as the explicit functions of the temperature:

$$qa \approx \frac{1}{\sqrt[3]{2\pi}}e^{-Ca^2\varepsilon_*^2/(3k_B T_b)}, \quad p_T \approx \frac{\sqrt{Ck_B T_b}}{\sqrt[6]{2\pi}}e^{-Ca^2\varepsilon_*^2/(6k_B T_b)}. \quad (13)$$

According to formula (13) the dependence of the thermal pressure on temperature is strongly nonlinear. We note that for crystals with smooth interactions such nonlinearity is not typical. Usually the dependence $p_T(T_b)$ is close to linear and

it is well described by the Mie-Gruneisen equation of state (see, e.g., [29,30]). Strongly nonlinear pressure-temperature dependence is usually observed in systems close to instability [29,31]. We also note that the thermal expansion coefficient, proportional to dp_T/dT_b, tends to zero as $T_b \to 0$. Similar temperature dependence of the thermal expansion coefficient is observed in real experiments and attributed to quantum effects (see, e.g., [32]). For $T_b > 0$ the thermal expansion coefficient is finite. Therefore under the initial conditions (5), thermoelastic effects such as the ballistic resonance [13] may occur. In the present paper, we ignore these effects and focus on the heat transfer. Investigation of thermoelastic effects requires a separate study.

We note that the density of breaks is sensitive to a small variation of temperature. Consider, for example, the densities of breaks at temperatures T_b and $T_b + \Delta T$. Using formula (13), we obtain for $\Delta T \ll T_b$

$$\frac{q(T_b + \Delta T)}{q(T_b)} \approx \exp\left(\frac{Ca^2\varepsilon_*^2}{3k_B T_b}\frac{\Delta T}{T_b}\right) = (\sqrt[3]{2\pi}aq(T_b))^{-\Delta T/T_b}. \quad (14)$$

Here $\frac{Ca^2\varepsilon_*^2}{3k_B T_b}$ is a large parameter, while $\Delta T/T_b$ and $aq(T_b)$ are small parameters. Formula (14) shows that $q(T_b + \Delta T)/q(T_b)$ strongly depends on $\Delta T/T_b$. This fact should be taken into account in numerical experiments.

Formulas (9)–(13) allow one to estimate the density of breaks at a given temperature. To check the accuracy of these formulas, the equations of motion (1) with initial conditions (5) and $T_0(x) = T_b = $ const (uniform temperature profile) are solved numerically. The solution of equations of motion (1) is carried out under periodic boundary conditions (2) using two numerical schemes. Both schemes are based on the following central difference approximation:

$$v_n\left(t + \frac{\Delta\tau}{2}\right) = v_n\left(t - \frac{\Delta\tau}{2}\right) + \frac{\Delta\tau}{m}(F_{n+1} - F_n),$$

$$u_n(t + \Delta\tau) = u_n(t) + v_n\left(t + \frac{\Delta\tau}{2}\right)\Delta\tau, \quad (15)$$

where $v_n = \dot{u}_n$, $\Delta\tau$ is the time step. In the first scheme, the discontinuous interparticle force (1) is modified for relative displacements $u_n - u_{n-1}$ in the interval $[a\varepsilon_* - 2\bar{v}\Delta\tau, a\varepsilon_* + 2\bar{v}\Delta\tau]$, where $\bar{v}$ is the root-mean-squared particle velocity, corresponding to the background temperature T_b. In this interval the force is replaced by a continuous piecewise linear function such that for $|u_n - u_{n-1} - a\varepsilon_*| < 2\bar{v}\Delta\tau$

$$F_n = C\left(\frac{a\varepsilon_*}{4\bar{v}\Delta\tau} - \frac{1}{2}\right)(u_{n-1} - u_n + a\varepsilon_* + 2\bar{v}\Delta\tau). \quad (16)$$

The second numerical scheme explicitly accounts for bond dissociation during the integration step. Before each step, it is predicted whether the bond will dissociate or form during this step. To predict these events, the time, t_{br}, at which the interparticle force reaches the maximum value $Ca\varepsilon_*$ is estimated as

$$t_{br} - t \approx \frac{a\varepsilon_* - u_{n+1}(t) + u_n(t)}{v_{n+1}(t - \Delta\tau/2) - v_n(t - \Delta\tau/2)}. \quad (17)$$

If $|t_{br} - t| > \Delta\tau/2$, then none of the events occur and the integration step is performed using the formulas (15). Otherwise,

---

[2]The strain distribution function is defined such that $\zeta(\varepsilon)\Delta\varepsilon$ is equal to the probability of observing the strain in the interval $[\varepsilon; \varepsilon + \Delta\varepsilon]$.
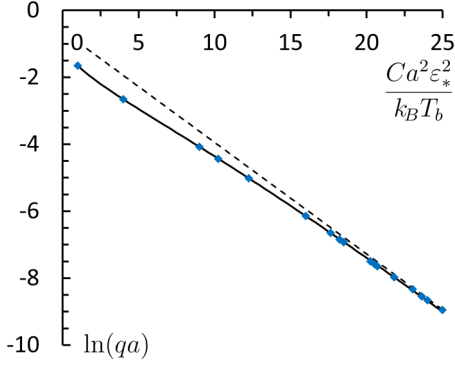
FIG. 1. Temperature dependence of the average density of breaks in the uniformly heated chain. The exact analytical solution (9)–(12) (solid line), approximate solution (13) (dashed line), and results of numerical simulations (points) are shown.

the formulas (15) for u_n, v_n are corrected including values of order of $\Delta\tau^2$. In all further simulations, the results obtained by the two numerical schemes practically coincide. For both numerical schemes small drift of the total energy of the chain was observed. However, the rate of increase of the total energy was at an acceptable level—of the order of 0.1% per 10^7 time steps.

To calculate the temperature dependence of the density of breaks, the following values of parameters are used:

$$N = 5 \times 10^4, \quad N_r = 1.4 \times 10^3, \quad \frac{\Delta\tau}{\tau_*} = \frac{1}{120}, \quad (18)$$

where N is the number of particles, N_r is the number of realizations, and $\tau_* = 2\pi\sqrt{m/C}$. Dependence of the density of breaks, averaged over time and realizations, on the parameter $Ca^2\varepsilon_*^2/(k_B T_b)$ is shown in Fig. 1. It is seen that the analytical solution (9)–(12) coincides with the numerical results. In the case of low density of breaks (small temperatures), simplified formula (13) can be used. Further, formulas (9)–(13) are used for choosing the temperature T_b and other parameters of the chain, corresponding to the desired density of breaks q.

III. GAS WITH BARRIERS AS A KINETIC MODEL OF HEAT TRANSFER

A. Kinetic equation for a gas with barriers

In the present section, a kinetic model of heat transfer is developed. The heat transfer is modeled by a motion of quasiparticles, carrying energy. It is assumed that bond dissociation causes elastic reflection of the quasiparticles. From a mathematical point of view, velocities of quasiparticles change sign with a certain probability, proportional to the density of breaks q. Between reflections, quasiparticles move with constant speed.

Consider the motion of noninteracting quasiparticles (ideal gas) in a one-dimensional channel. Distribution of coordinates and velocities of the qusiparticles at time t is described by the distribution function $f(t, x, v)$ defined as

$$f(t, x, v) = \lim_{\Delta x, \Delta v \to 0} \frac{\Delta N(t, x, v)}{\Delta x \Delta v}, \quad (19)$$

where $\Delta N(t, x, v)$ is the number of quasiparticles having at time t coordinates in the interval $[x; x + \Delta x]$ and velocities in the interval $[v; v + \Delta v]$. We assume that each quasiparticle carries the same amount of thermal energy. Then temperature $T(t, x)$ is proportional to gas density $\rho(t, x)$ (number of quasiparticles per unit length in the vicinity of point x at time t), while the heat flux $h(t, x)$ is proportional to the flux of quasiparticles, i.e.,

$$T(t, x) = \frac{\rho(t, x)}{\gamma_1} = \frac{1}{\gamma_1} \int_{-\infty}^{\infty} f(t, x, v) \, dv,$$

$$h(t, x) = \frac{\gamma_2}{\gamma_1} \int_{-\infty}^{\infty} f(t, x, v) v \, dv, \quad (20)$$

where γ_1, γ_2 are dimensional proportionality coefficients.

To derive the balance equation, describing the evolution of the distribution function $f(t, x, v)$, we consider changes in number of quasiparticles with coordinates and velocities in the intervals $[x; x + \Delta x]$, $[v; v + \Delta v]$ from time t to $t + \Delta t$:

$$(f(t + \Delta t, x, v) - f(t, x, v))\Delta x \Delta v$$
$$= (f(t, x, v) - f(t, x + \Delta x, v))v\Delta t \Delta v$$
$$- P(t, x, v) \Delta t f(t, x, v)\Delta x \Delta v$$
$$+ P(t, x, -v)\Delta t f(t, x, -v)\Delta x \Delta v, \quad (21)$$

where $P(t, x, v) \Delta t$ is the probability for a quasiparticle to be reflected during the interval Δt. Series expansion of f with respect to Δx, Δv, Δt in Eq. (21), yields

$$\dot{f}(t, x, v) = -vf'(t, x, v) + P(t, x, -v)f(t, x, -v)$$
$$- P(t, x, v)f(t, x, v), \quad (22)$$

where the overdot stands for time derivative and the prime stands for spatial derivative. If the function $P(t, x, v)$ is known, then Eq. (22) is closed. In general, the function $f(t, x, v)$ depends on three variables. However, the derivative of $f(t, x, v)$ with respect to v is absent in Eq. (22), and therefore v can be considered as a parameter of this equation.

We note that integrating (22) with respect to the velocities of the quasiparticles and using formulas (20), yields the following balance equation:

$$\gamma_2 \dot{T} = -h'. \quad (23)$$

This equation has the same form as the heat conduction equation for a medium with constant heat capacity. Using the distribution function for deformation (9), it can be shown that the heat capacity of the chains with breaks depends on temperature. However, we further assume that under conditions (8) this dependence can be neglected in the first approximation.

To obtain a closed equation for the distribution function $f(t, x, v)$, we assume that the probability of reflection $P(t, x, v)\Delta t$ is independent of time and spatial coordinates. The probability is calculated as a density of breaks q multiplied by the distance $|v|\Delta t$ traveled by a quasiparticle, i.e.,

$$P(t, x, v) \Delta t = q |v|\Delta t. \quad (24)$$

We note that according to (24), q is inversely proportional to the mean free path of the quasiparticle, i.e., $q = 1/l_{\mathrm{mfp}}$.

Substitution of (24) into Eq. (22) yields

$$\dot{f} + vf' = q|v|(f^* - f), \quad f(t, x, v)^* = f(t, x, -v). \quad (25)$$

A similar equation is derived for f^*. Then excluding f^*, we obtain

$$\ddot{f} + 2q|v|\dot{f} = v^2 f''. \qquad (26)$$

Therefore the evolution of the distribution function is governed by Eq. (26) of a telegraph type.

In the general case, the initial conditions for Eq. (22) have the form

$$f(0, x, v) = f_0(x, v), \qquad (27)$$

where $f_0(x, v)$ is the initial distribution function. We assume that the quasiparticles move in an infinite space or a periodic domain. The initial conditions for Eq. (26), corresponding to (27), are obtained using Eq. (25):

$$f(0, x, v) = f_0, \quad \dot{f}(0, x, v) = -v f_0' + q|v|(f_0^* - f_0). \quad (28)$$

Further, we mostly focus on the following particular case of (28):

$$f_0(x, v) = \rho_0(x)\phi(v) = \gamma_1 T_0(x)\phi(v),$$

$$\int_{-\infty}^{\infty} \phi(v)dv = 1, \quad \phi(-v) = \phi(v), \qquad (29)$$

where $\rho_0(x) = \rho(0, x)$, $T_0(x) = T(0, x)$ are the initial density and the corresponding initial temperature, and $\phi(v)$ is the initial velocity distribution of quasiparticles such that $\phi(v)\Delta v$ is proportional to the number of quasipartices with velocities in the interval $[v; v + \Delta v]$ [see, e.g., formula (91)]. Since function $\phi(v)$ is even, initial fluxes are absent[3] (initial conditions with nonzero flux are considered in Sec. VII). In Sec. VIII it is shown that under initial conditions (29) there is a direct relation between an initial problem for motion of quasiparticles and a heat transfer problem (at least in a harmonic case). In particular, it is shown that function ϕ is determined by the relation between the group velocity and the wave number for a considered crystal.

Thus in the framework of kinetic theory, the heat transfer in the chain with breaks is described by the initial problem (26),(28),(29) with respect to the distribution function $f(t, x, v)$. Given the known distribution function, the temperature profile is calculated using formula (20).

B. Solution of the kinetic equation

We derive an exact solution of the initial problem (26),(28),(29). Since Eq. (26) is linear, it is sufficient to find its fundamental solution $\hat{f}(t, x, v)$, i.e., the solution under initial conditions $f(0, x, v) = \delta(x)$, $\dot{f}(0, x, v) = -v\delta'(x)$. Using the known solution of the telegraph equation (see, e.g., [33]), we obtain[4]

$$\hat{f}(t, x, v) = e^{-q|v|t}\delta(x - vt) + \frac{q}{2}e^{-q|v|t}$$

$$\times \left(\mathrm{sgn}(v)\frac{x + vt}{\sqrt{z}} I_1(q\sqrt{z}) + I_0(q\sqrt{z}) \right)\theta(z),$$

$$z = v^2 t^2 - x^2, \qquad (30)$$

where I_0, I_1 are modified Bessel functions of the first kind.

The general solution for the distribution function $f(t, x, v)$ is obtained by convolution of the fundamental solution (30) and the initial temperature distribution $T_0(x)$:

$$f(t, x, v) = \gamma_1 \int_{-\infty}^{\infty} \hat{f}(t, \xi, v) T_0(x - \xi)\phi(v)d\xi$$

$$= \gamma_1 e^{-q|v|t}\phi(v)\left[T_0(x - vt) + \frac{q}{2}\int_{x-vt}^{x+vt} T_0(x - \xi) \right.$$

$$\left. \times \left(\mathrm{sgn}(v)\frac{\xi + vt}{\sqrt{z}} I_1(q\sqrt{z}) + I_0(q\sqrt{z}) \right)d\xi \right],$$

$$z = v^2 t^2 - \xi^2. \qquad (31)$$

The corresponding temperature profile can be obtained using Eq. (20). Further, we analyze several particular cases of the general solution (31).

IV. FUNDAMENTAL SOLUTION FOR TEMPERATURE

In this section, we analyze the behavior of the temperature profile $\hat{T}(t, x)$ corresponding to $T_0 = \delta(x)$ and $\phi(v) = \phi(-v)$, which is further referred to as the fundamental solution for temperature. In particular, we investigate the transition from the ballistic to the diffusive regime of heat transfer.

The fundamental solution for temperature $\hat{T}(t, x)$ is related to the fundamental solution (30) of the kinetic equation as

$$\hat{T}(t, x) \overset{\text{def}}{=} \int_{-\infty}^{\infty} \hat{f}(t, x, v)\phi(v)dv. \qquad (32)$$

For the known fundamental solution, the general solution with an arbitrary $T_0(x)$ is calculated as

$$T(t, x) = \int_{-\infty}^{\infty} \hat{T}(t, \xi) T_0(x - \xi)\,d\xi. \qquad (33)$$

We note that introducing the fundamental solution $\hat{T}$ and representing temperature through its initial distribution $T_0(x)$ is only possible under multiplicative initial conditions (29).

The velocities of the quasiparticles and function $\phi(v)$ in (32) are chosen as

$$v = c_g(\kappa), \quad d\kappa = -\phi(v)dv. \qquad (34)$$

In Sec. VIII, it is shown that formula (34) guarantees that the solution of the kinetic equation in the ballistic limit coincides with the expression describing heat transfer in the Hooke chain under initial conditions (5) (see, e.g., papers [11,12]).

Substituting the expression (30) for $\hat{f}$ into (32), and changing the integration variable as in (34), we obtain

$$\hat{T}(t, x) = \int_0^1 e^{-q|c_g|t}\delta(x - c_g t)d\kappa$$

$$+ \frac{q}{2}\int_0^1 e^{-q|c_g|t}\left(\frac{|c_g|t}{\sqrt{z}} I_1(q\sqrt{z}) + I_0(q\sqrt{z}) \right)\theta(z)d\kappa,$$

$$z = c_g^2 t^2 - x^2. \qquad (35)$$

If the group velocity is given by formula (4), then the fundamental solution in dimensionless variables $\tilde{x} = qx$ and $\tilde{t} =$

---

[3]We note that this is a sufficient, but not necessary condition for the absence of fluxes.

[4]Note that these conditions correspond to zero initial flux.

qct, $\tilde{c}_g = c_g/c$ takes the form

$$\frac{\hat{T}}{q} = \frac{e^{-|\tilde{x}|}\theta(\tilde{t}^2 - \tilde{x}^2)}{\pi\sqrt{\tilde{t}^2 - \tilde{x}^2}} + \frac{1}{2}\int_0^1 e^{-|\tilde{c}_g|\tilde{t}}$$

$$\times \left[\frac{|\tilde{c}_g|\tilde{t}}{\sqrt{\tilde{z}}}I_1(\sqrt{\tilde{z}}) + I_0(\sqrt{\tilde{z}})\right]\theta(\tilde{z})d\kappa, \qquad (36)$$

where $\tilde{z} = \tilde{c}_g^2\tilde{t}^2 - \tilde{x}^2$. Formula (36) shows that $\hat{T}/q$ depends on the density of breaks q only through the scaling of coordinate and time. Therefore the behavior of the dimensionless fundamental solution in chains with different densities of breaks is identical.

Further in this section, we analyze the behavior of the fundamental solution for temperature (36).

A. Transfer function and shape function

To simplify the analysis of the fundamental solution for temperature, we introduce two single-variable functions referred to as the transfer function and the shape function. These functions allow one, in particular, to distinguish ballistic, diffusive, and anomalous heat transfer regimes.

The transfer function is defined as

$$r(t) \stackrel{\text{def}}{=} \left(\int_{-\infty}^{\infty} x^2\hat{T}(t, x)dx\right)^{1/2}. \qquad (37)$$

This function shows how far the initial disturbance, initially localized at $x = 0$, spreads over time t. We note that this function is finite even when the "front" propagates with infinite speed (as in the case of the Fourier heat conduction).

Using the transfer function, we rigorously define ballistic, anomalous, and diffusive regimes of heat transfer. The transfer functions, corresponding to these regimes, are denoted as r_a, r_b, and r_d. In the ballistic regime, the transfer function is linear in time:

$$r_b(t) = \bar{c}t, \qquad (38)$$

where $\bar{c}$ is the root-mean-square velocity of quasiparticles [see (48)]. In the diffusive regime, the transfer function is proportional to the square root of time:

$$r_d(t) = \sqrt{2\bar{b}t}, \qquad (39)$$

where $\bar{b}$ is the effective diffusion coefficient, independent of time. In literature, the anomalous heat transfer regime is also introduced (see, e.g., paper [7]). In this regime, the transfer function has the form [34]

$$r_a(t) \sim t^{\alpha}, \quad \frac{1}{2} < \alpha < 1. \qquad (40)$$

To calculate the coefficients $\bar{c}, \bar{b}$ in numerical simulations, the formulas, following from (38) and (39), can be used:

$$\bar{c} = \frac{r(t)}{t}, \quad \bar{b} = \frac{r^2(t)}{2t}, \qquad (41)$$

where $r(t)$ is calculated using (37). If the regime of heat transfer is purely ballistic or purely diffusive, then coefficients $\bar{c}, \bar{b}$ are time independent.

To describe the spatial distribution of temperature, we introduce the shape function defined as

$$g(t, s) \stackrel{\text{def}}{=} r(t)\hat{T}(t, r(t)s). \qquad (42)$$

Here and below s is a dimensionless coordinate. The shape function satisfies the relations, following from the properties of the fundamental solution:

$$\int_{-\infty}^{\infty} g(t, s)ds = \int_{-\infty}^{\infty} s^2 g(t, s)ds = 1. \qquad (43)$$

If the fundamental solution can be represented as

$$\hat{T}(t, x) = \frac{1}{r(t)}g\left(\frac{x}{r(t)}\right), \qquad (44)$$

the shape function is time independent, i.e., $g(t, s) \equiv g(s)$. Then using formula (44), we rewrite the general solution (33), corresponding to an arbitrary $T_0(x)$, via $r(t)$ and $g(s)$ as

$$T(t, x) = \int_{-\infty}^{\infty} g(s)T_0(x - r(t)s)ds. \qquad (45)$$

This formula is further used in Sec. V.

Thus introducing the transfer and the shape functions allows one to simplify the analysis of the fundamental solution. Instead of analyzing the function of two variables $\hat{T}(x, t)$, two single-variable functions $r(t)$ and $g(s)$ are considered. Examples of these functions for ballistic and diffusive regimes are given below [see formulas (48) and (54)]. We note that the ballistic and diffusive regimes may correspond to the same shape function. In this case, for the same initial conditions, identical spatial distributions of temperature are realized, but at different moments in time.

B. Ballistic limit

The ballistic heat transfer is realized either in the absence of breaks ($q = 0$) or at sufficiently small times ($qct \ll 1$). In these cases, the kinetic equation (25) and its solution with initial conditions (29) take the form

$$\dot{f} + vf' = 0 \rightarrow f(t, x, v) = \gamma_1 T_0(x - vt)\phi(v). \qquad (46)$$

Then using formulas (20), we obtain the expression for temperature

$$T(t, x) = \int_{-\infty}^{\infty} T_0(x - vt)\phi(v)dv$$

$$= \int_0^1 T_0(x - c_g(\kappa)t)d\kappa. \qquad (47)$$

The relation between the two integrals in formula (47) is discussed in Sec. VIII. The fundamental solution, the transfer function $r_b(t)$, and the shape function $g_b(s)$, corresponding to (47), have the form

$$\hat{T}(t, x) = \frac{1}{r_b(t)}g_b\left(\frac{x}{r_b(t)}\right), \quad g_b(s) = \bar{c}\phi(\bar{c}s),$$

$$r_b(t) = \bar{c}t, \quad \bar{c}^2 = \int_{-\infty}^{\infty} v^2\phi(v)dv = \int_0^1 c_g^2 d\kappa. \qquad (48)$$

It is seen that the shape function is determined by the initial velocity distribution of quasiparticles ϕ. The transfer function is linear in time as it should be in the ballistic regime of heat transfer.
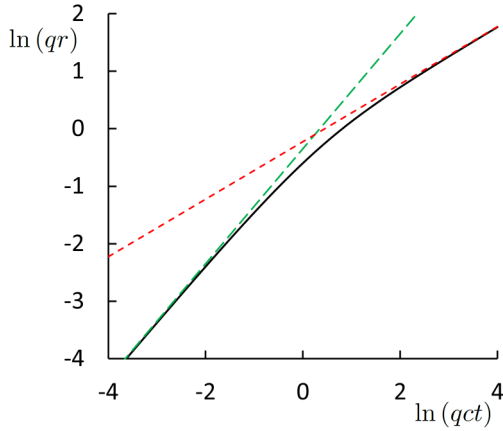
FIG. 2. Logarithm of the transfer function. The exact solution (36) of the kinetic equation (solid line), the ballistic limit $r_b = \bar{c}t$ (green dashed line), and the diffusive limit $r_d = \sqrt{2\bar{b}t}$ (red dashed line) are shown. Parameters $\bar{c}$ and $\bar{b}$ are determined by formulas (49) and (55). The dashed lines intersect at $qct = 4/\pi$.

If the group velocity is given by (4) (for the Hooke chain), functions (48) for g_b and $\bar{c}$ take the form

$$g_b(s) = \frac{\theta(2 - s^2)}{\pi\sqrt{2 - s^2}}, \quad \bar{c} = \frac{c}{\sqrt{2}}. \tag{49}$$

In the absence of breaks ($q = 0$), formulas (48) and (49) yield the exact solution of the kinetic equation, while for nonzero q the formulas give reasonable approximation of the solution at small times, i.e., $qct \ll 1$ (see Figs. 2 and 3).

C. Diffusive limit

We consider the approximation of the fundamental solution $\hat{T}$ at large times far from the ballistic fronts. This solution has diffusive character, i.e., the corresponding transfer function is proportional to $\sqrt{t}$.

According to formula (30), the fundamental solution of the kinetic equation $\hat{f}$ for any fixed v has fronts at $x = \pm vt$. We
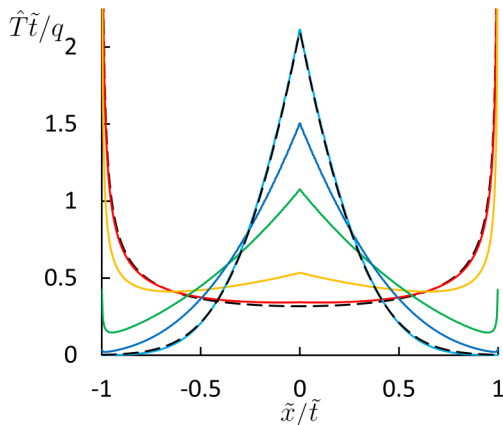

FIG. 3. Fundamental solution for temperature (36) at $\tilde{t} = qct = 0.05$ (red), 0.5 (orange), 2.5 (green), 5 (blue), and 10 (light blue). Dashed lines correspond to the ballistic limit [formula (49)] and the diffusive limit [formula (53) at $\tilde{t} = 10$].

consider the behavior of $\hat{f}$ at large times far from the fronts, i.e., for

$$q|v|t \gg 1, \quad |x| \ll |v|t. \tag{50}$$

Note that as the time t increases, the conditions (50) are satisfied for an increasing number of quasiparticles (larger range of velocities v), hence the accuracy of the approximate solution obtained below increases with time.

The conditions (50) allow one to neglect the delta function in (30), because it is equal to zero everywhere except for the fronts. We also use the asymptotics of the Bessel function $I_\nu(u) \approx e^u/\sqrt{2\pi u}$, valid for large u, and use the approximation $\sqrt{v^2 t^2 - x^2} \approx |v|t - x^2/(2|v|t)$, valid under conditions (50). Then from (30) it follows that the fundamental solution has the form

$$\hat{f}(t, x, v) \approx \sqrt{\frac{q}{2\pi|v|t}} e^{-qx^2/(2|v|t)}. \tag{51}$$

It is seen that the fundamental solution of the kinetic equation has the same form as the solution of the Fourier heat conduction equation. Therefore if all quasiparticles had the same velocity, then the Fourier law would be satisfied. Evidently, in the chain with breaks it is not the case, because the quasiparticles have different velocities due to dispersion.

We note that the approximate solution (51) can also be derived from (26). Neglecting the second time derivative in Eq. (26), we obtain the diffusion equation

$$\dot{f} = \frac{|v|}{2q} f''. \tag{52}$$

The fundamental solution of this equation coincides with (51). This approach is shorter, however it does not yield the conditions (50), under which the approximate solution (51) is valid.

Using formula (51), we derive the fundamental solution for temperature $\hat{T}$ in the diffusive limit. Substituting (51) into (32) and using the fact that functions $\hat{f}$ and ϕ are even with respect to v, yields

$$\hat{T}(t, x) \approx \sqrt{\frac{2q}{\pi t}} \int_0^\infty \frac{e^{-qx^2/(2vt)}}{\sqrt{v}} \phi(v) dv$$
$$= \sqrt{\frac{q}{2\pi t}} \int_0^1 \frac{e^{-qx^2/(2|c_g|t)}}{\sqrt{|c_g|}} d\kappa. \tag{53}$$

Here the second formula follows from the first one, provided that the substitution $v = c_g(\kappa)$ is made (see Sec. VIII). In the first formula from (53) integration is carried out with respect to all velocities v, including small velocities for which the conditions (50) are not satisfied. However, the contribution of these velocities to the temperature decreases with time. This fact is demonstrated in the next subsection (see Fig. 3).

To analyze the fundamental solution (53), we represent it in the form (44) using the transfer function $r_d(t)$ and the shape function $g_d(s)$. In turn, the diffusive shape function g_d is represented via the ballistic shape function g_b using formulas

(37), (42), and (53):

$$\hat{T}(t, x) = \frac{1}{r_d(t)} g_d\left(\frac{x}{r_d(t)}\right),$$

$$g_d(s) = \sqrt{\frac{4\psi}{\pi}} \int_0^\infty \frac{e^{-\psi s^2/z}}{\sqrt{z}} g_b(z) dz,$$

$$r_d(t) = \sqrt{2\bar{b}t}, \quad \bar{b} = \frac{\psi \bar{c}}{q}, \quad \psi = \int_0^\infty z g_b(z) dz, \quad (54)$$

where $\bar{b}$ is the effective diffusion coefficient. The possibility of representing the diffusive characteristics g_d and $\bar{b}$ via the ballistic shape function g_b is due to the fact that g_b is proportional to the initial velocity distribution of quasiparticles $\phi(v)$ [see formula (48)], which in turn affects the diffusive transport. If the group velocity is given by the formula (4), the shape function and the diffusion coefficient in the formula (54) can be expressed as

$$g_d(s) = \frac{\sqrt{2}}{\pi^3} |s| K_{1/4}^2\left(\frac{s^2}{2\pi}\right), \quad \bar{b} = \frac{c}{\pi q}, \quad (55)$$

where K is the modified Bessel function of the second kind.

We compare the transfer function (54) and the shape function (55) for the chain with breaks, with similar functions for the Fourier thermal conductivity, described by the equation $\dot{T} = \beta T''$. Here β is the thermal diffusivity. The fundamental solution of this equation, the corresponding transfer function r_F, and shape function g_F have the form

$$\hat{T}_F(t, x) = \frac{1}{r_F(t)} g_F\left(\frac{x}{r_F(t)}\right), \quad r_F(t) = \sqrt{2\bar{b}t},$$

$$g_F(s) = \frac{1}{\sqrt{2\pi}} e^{-s^2/2}, \quad \bar{b} = \beta. \quad (56)$$

A comparison of formulas (53), (55), and (56) shows that the transfer functions $r_d(t)$ and $r_F(t)$ have the same form. However, the shape function $g_d(s)$ is generally different from the Gaussian function $g_F(s)$, which is characteristic of classical Fourier thermal conductivity. In particular, the shape function $g_d(s)$ (55) has a kink (discontinuity of the first derivative) at $s = 0$ (see Fig. 3), while the Gaussian function $g_F(s)$ (56) has zero derivative at this point. This difference is crucial, because in isolated systems, obeying the Fourier law, temperature profiles with kinks are not possible in principle (discontinuity in the derivative of temperature leads to the discontinuity in the heat flux, which is forbidden by the law of energy balance for an isolated system).

This result may seem unexpected, since the distribution function (51) in the problem under consideration is described by the Gaussian function and the classical diffusion equation (52). Indeed, for each group velocity v, the process is described by the diffusion equation (52), but with a coefficient depending on v. The summation of solutions of these equations with respect to v yields a curve different from the Gaussian. The reason for this behavior of the system lies in the fact that in the considered model, the processes, described by different group velocities, are independent.

Thus, at large times, the reflection of quasiparticles from barriers (dissociated bonds) leads to a diffusive regime of heat transfer with a transfer function proportional to the square root

of time. The effective coefficient of thermal conductivity in this case is finite as in the paper [17] (see Sec. V). However, the shape function (55) differs significantly from the Gaussian curve, so the Fourier law is not satisfied.

D. Transition from ballistic to diffusive regime

The solutions obtained above show that the ballistic regime of heat transfer is realized in the system at small times, and the diffusive regime is realized at large times. We show below how the fundamental solution changes during the transition.

Using the fundamental solution (36), we show that the dimensionless transfer function qr depends only on the dimensionless time qct. The transfer function calculated using the solution (36) is shown in Fig. 2. For comparison, the plot also shows the transfer functions for the ballistic and diffusive limits, calculated by the formulas (49) and (55) (dashed lines). It can be seen from Fig. 2 that at small times the transfer function, corresponding to the exact solution, is proportional to t, and at large times it is proportional to $\sqrt{t}$. Therefore, there is a transition from the ballistic to the diffusive regime of heat transfer.

The time of transition from the ballistic regime to diffusive can be estimated by calculating the intersection point of the curves $r_b(t)$ and $r_d(t)$. Using (49) and (55), we get

$$qct_{\text{trans}} = \frac{4}{\pi}. \quad (57)$$

For $t < t_{\text{trans}}$ the exact transfer function is closer to the ballistic limit, while for $t > t_{\text{trans}}$ it is closer to the diffusive limit.

The fundamental solution is shown in Fig. 3. It is seen that at small times the heat transfer is almost ballistic and the fundamental solution is well described by the formulas (49) obtained in the ballistic limit. Most of the energy is concentrated near the fronts propagating at the speed of sound c. At lager times, the diffusive nature of the heat transfer begins to prevail, and most of the energy remains in the vicinity of the center. For $qct > 5$, almost all energy is transferred in a diffusive manner, and the fundamental solution becomes close to the formula (53) obtained in the diffusive limit. Note that the ballistic fronts at $x = \pm ct$ are formally present at any t. However, at large times they become very narrow and their contribution to heat transfer decreases.

Thus, the fundamental solution (36) describes the transition from the ballistic regime of heat transfer, which is realized at small times $qct \ll 1$, to the diffusive (non-Fourier) regime at large times $qct \gg 1$.

V. THE TRANSFER FUNCTION AND LENGTH DEPENDENCE OF EFFECTIVE THERMAL CONDUCTIVITY

In one-dimensional chains, the Fourier law is usually not satisfied and the effective thermal conductivity diverges, i.e., tends to infinity with increasing length (see, e.g., [7]). In the literature, this dependence is mainly determined in the nonequilibrium steady-state formulation (stationary heat transfer problem for a finite chain connected to two thermal reservoirs having different temperatures is considered). Using this formulation, in paper [17] it is shown that bond dissociation leads to a convergence of the effective thermal

conductivity to a finite value. In the present section, a similar result is obtained in the unsteady formulation. We show, in particular, that in the unsteady formulation, the dependence of the effective thermal conductivity on the length is directly related to the characteristics of the transfer function (37) and does not depend on the shape function (42).

Using the approach described in [28], we consider the heat transfer problem with the initial temperature profile

$$T_0(x) = T_b + \Delta T \theta(x), \tag{58}$$

where T_b, $T_b + \Delta T$ are initial temperatures of the left ($x < 0$) and the right ($x > 0$) parts of the chain. We define the effective thermal conductivity as the mean flux in the system divided by the mean temperature gradient, e.g.,

$$\mu = -\frac{\int_{-\infty}^{+\infty} h(t,x)dx}{\Delta T}. \tag{59}$$

From the energy balance equation (23) it follows that the following relation holds between the flux and the temperature profile (see also paper [28]):

$$h(t,x) = -\gamma_2 \int_{-\infty}^{x} \dot{T} \, dx. \tag{60}$$

Substituting the initial temperature profile (58) into formula (45), we obtain

$$T(t,x) = T_b + \Delta T \int_{-\infty}^{+\infty} \theta(x - r(t)s)g(s)ds,$$
$$\dot{T} = -\Delta T g\left(\frac{x}{r}\right)\frac{\dot{r}}{r}. \tag{61}$$

Substituting (60) and (61) into formula (59) yields the expression for the effective thermal conductivity:

$$\mu = -\frac{\gamma_2}{2}\frac{d}{dt}(r^2)\int_{-\infty}^{+\infty}\int_{-\infty}^{s} g(s)ds \sim \frac{d}{dt}(r^2). \tag{62}$$

In particular, for the power-law dependence of the transfer function on time $r(t) \sim t^p$ the thermal conductivity has the form

$$\mu \sim r^{(2p-1)/p} \tag{63}$$

Formula (63) can be considered as the length dependence of the effective thermal conductivity in the unsteady problem. The exponent in this dependence $(2p-1)/p$ is determined by the exponent p in time dependence of the transfer function. We note that a similar relation between these two exponents is obtained by different means in paper [34].

Formulas (62) and (63) show that the effective thermal conductivity does not depend on time only if $r(t) \sim \sqrt{t}$. As shown above, in the chain with breaks, such a time dependence of the transfer function is realized at $qct \gg 1$. Therefore, for this system, the effective thermal conductivity converges to a finite value.

Note that the shape function does not affect the length dependence of the thermal conductivity. Therefore, the absence of this dependence, generally, does not guarantee the fulfillment of the Fourier law. In particular, for the chain with breaks, the effective thermal conductivity in the diffusive limit does not depend on the length, but the Fourier law is not satisfied.

VI. EXAMPLE: SINUSOIDAL TEMPERATURE PROFILE

In this section, we check how accurately the kinetic model reproduces the results of the numerical integration of equations of motion (1) for the chain with breaks with the initial conditions (5). The comparison is carried out using the example problem with sinusoidal initial temperature profile

$$T_0(x) = T_b + B_0 \sin(\lambda x), \quad \lambda = \frac{2\pi}{L}, \tag{64}$$

where L is the wavelength of sine, T_b is the background temperature, and $B_0 < T_b$ is the initial amplitude of sine. This profile is chosen for two reasons. First, it can be implemented in experiments based on the transient thermal grating technique [35–37]. Second, as shown below, the temperature profile remains sinusoidal. As a result, only the time dependence of the amplitude of sine can be considered, which significantly reduces the number of realizations required to achieve acceptable accuracy.

A. Analytical solution

We construct an analytical solution of the heat transfer problem, corresponding to the sinusoidal initial temperature profile (64). In this case, the initial conditions are given by formulas (28) and (29) with the initial distribution function

$$f_0 = \gamma_1(T_b + B_0 \sin(\lambda x))\phi(v). \tag{65}$$

Substituting expression (65) into formula (31) and taking into account the properties of the fundamental solution (30), we obtain

$$T(t,x) = T_b + B(t)\sin(\lambda x),$$
$$B(t) = B_0 \int_{-\infty}^{\infty}\int_{-\infty}^{\infty} \hat{f}(\xi, v, t)\cos(\lambda\xi)\phi(v)d\xi \, dv. \tag{66}$$

It is seen that the temperature distribution remains sinusoidal. Substituting the fundamental solution (30) into (66), we show that the temperature amplitude B varies with time according to the formulas

$$B(t) = B_b(t) + B_d(t),$$
$$B_b(t) = B_0 \int_{-\infty}^{\infty} e^{-q|v|t}\cos(\lambda vt)\phi(v)dv,$$
$$B_d(t) = \frac{B_0 q}{2}\int_{-\infty}^{\infty} e^{-q|v|t}\phi(v)\int_{-vt}^{vt}\left(\frac{|v|t}{\sqrt{z}}I_1(q\sqrt{z})\right.$$
$$\left. + I_0(q\sqrt{z})\right)\cos(\lambda\xi)d\xi \, dv, \quad z = v^2t^2 - \xi^2. \tag{67}$$

Changing the integration variable in (67) as described in Sec. VIII, yields

$$B_b(t) = B_0 \int_0^1 e^{-q|c_g|t}\cos(\lambda c_g t)d\kappa,$$
$$B_d(t) = \frac{B_0 q}{2\lambda}\int_0^1 e^{-q|c_g|t}\int_{-\lambda c_g t}^{\lambda c_g t}\left[\frac{\lambda|c_g|t}{\sqrt{z_1}}I_1\left(\frac{q\sqrt{z_1}}{\lambda}\right)\right.$$
$$\left. + I_0\left(\frac{q\sqrt{z_1}}{\lambda}\right)\right]\cos\xi \, d\xi \, d\kappa, \quad z_1 = \lambda^2 c_g^2 t^2 - \xi^2. \tag{68}$$

It is seen from formula (68) that B_b and B_d depend on the dimensionless time $\tilde{t} = qct$ and the dimensionless density of breaks q/λ. Therefore, in further calculations we fix λ and change only q.

If the group velocity is given by the formula (4), the integrals in formula (68) can be expressed in terms of special functions. For the case ($q \neq \lambda$), formula (68) takes the form

$$B(t) = \frac{B_0}{2}\left[Q(\tau_+) + Q(\tau_-) - \frac{Q(\tau_+) - Q(\tau_-)}{\sqrt{1 - \lambda^2/q^2}}\right],$$

$$Q(\tau_\pm) = I_0(\tau_\pm) - L_0(\tau_\pm),$$

$$\tau_\pm = qct(1 \pm \sqrt{1 - \lambda^2/q^2}), \tag{69}$$

where L_0 is the modified Struve function. The case of small density of breaks corresponds to complex values $\tau_\pm$, while the case of large density of breaks corresponds to real values. Note that for a real argument, both functions I_0 and L_0 increase, while their difference decreases.

For small density of breaks $q/\lambda \ll 1$, formula (69) has the following asymptotics at large times:

$$\frac{B(t)}{B_0} \approx \sqrt{\frac{2q}{\pi \lambda \tilde{t}}} e^{-\tilde{t}} \cos\left(\frac{\lambda}{q}\tilde{t} - \frac{\pi}{4}\right) + \frac{4q^2}{\pi \lambda^2 \tilde{t}}. \tag{70}$$

Note that the two terms in the asymptotics have different order with respect to the small parameter q/λ and decay at different speeds.

For a large density of breaks $q/\lambda \gg 1$[5] the asymptotics of (69) takes the form

$$\frac{B(t)}{B_0} \approx \frac{4q^2}{\pi \lambda^2 \tilde{t}}. \tag{71}$$

The formulas (70) and (71) show that the decay of amplitude of sine is oscillatory at small densities of breaks, and monotonic at large densities of breaks. In the latter case, it is described by a power function, not an exponent. The latter fact once again demonstrates that the diffusion realized in the chain with breaks differs from the classical Fourier diffusion.

B. Numerical modeling

To check the analytical solution (68), it is compared with the results of numerical integration of the dynamic equations (1) with the initial conditions (5) and (64).

The initial conditions are set in two stages. At the first stage, the particles are given random velocities corresponding to the background temperature T_b. At the second stage (at $qct = 1$), a sinusoidal disturbance is added. Between the two stages the density of breaks increases from zero (at $t = 0$) to the equilibrium value corresponding to the background temperature.

In simulations, the temperatures of all particles in the chain are calculated by formula (7) and then used to determine the amplitude of sine $B(t)$ by formula

$$B(t) = \frac{2}{L}\int_0^L T(t, x)\sin(\lambda x)dx. \tag{72}$$

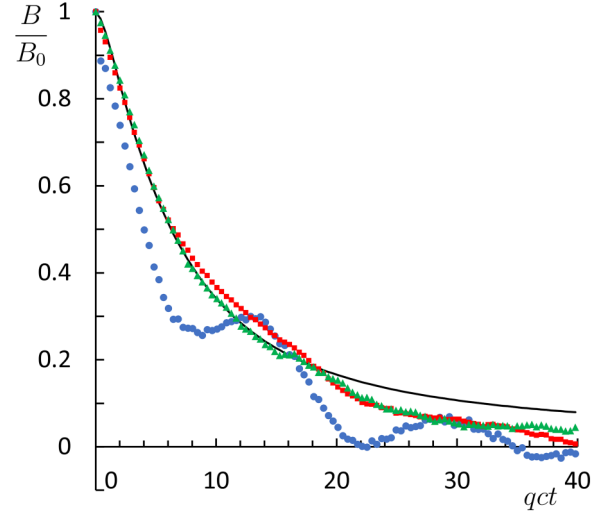[5]Here $Q(x) \sim \frac{2}{\pi x}$ is used.

FIG. 4. Time dependence of the amplitude of the sinusoidal temperature profile for chains of different length for $q/\lambda = 1.6$, $N_r = 1.4 \times 10^3$. Simulation results for $N = 10^3$ (circles), 10^4 (squares), 5×10^4 (triangles), and analytical solution (68) (solid line) are shown.

According to the analytical solution (68), the dimensionless amplitude of sine B/B_0 depends on dimensionless time qct and parameter q/λ. The numerical solution is more complicated as it additionally depends on B_0/T_b, N, and N_r. The parameter B_0/T_b should be taken as small as possible to minimize the variation of the density of breaks along the chain. We use the value $B_0/T_b = 0.05$. A further decrease of this parameter practically does not change the simulation results (see Fig. 7).

We fix $q/\lambda = 1.6$ and investigate the decay of the amplitude of sine $B(t)$ for chains containing different numbers of particles N. Note that as N increases, the density of breaks q decreases (for a fixed q/λ). Simulation results for $q/\lambda = 1.6$ and $N = 10^3, 10^4, 5 \times 10^4$ are shown in Fig. 4. It is seen that for $N = 10^3$ an oscillatory decay of the temperature is observed, while for $N = 10^4$ the decay is monotonic. A further increase in the number of particles does not qualitatively change the results. Therefore, for further calculations, we use $N = 10^4$ or $N = 5 \times 10^4$. Note that in the absence of breaks ($q = 0$), the convergence of the results with respect to the number of particles is significantly faster, and 10^2–10^3 particles is usually sufficient (see, e.g., the work [11]).

We consider the effect of the density of breaks on the decay of the sinusoidal temperature profile. The time dependence of the amplitude of sine for $q/\lambda = 2.7 \times 10^{-3}, 0.18, 2.7$ is shown in Figs. 5–7. At small densities of breaks (e.g., at $q/\lambda = 2.7 \times 10^{-3}$, Fig. 5) the decay of sine can be described approximately by a harmonic model in which the ballistic regime of heat transfer is realized. An increase in the density of breaks leads to a faster decay of temperature (Fig. 6). At large densities of breaks, the heat transfer is diffusive and the decay is monotonic (Fig. 7).

Thus, an increase in the density of breaks leads to a transition from the ballistic regime of heat transfer, which is characterized by the oscillatory decay of temperature, to the diffusive regime, corresponding to monotonic decay. This
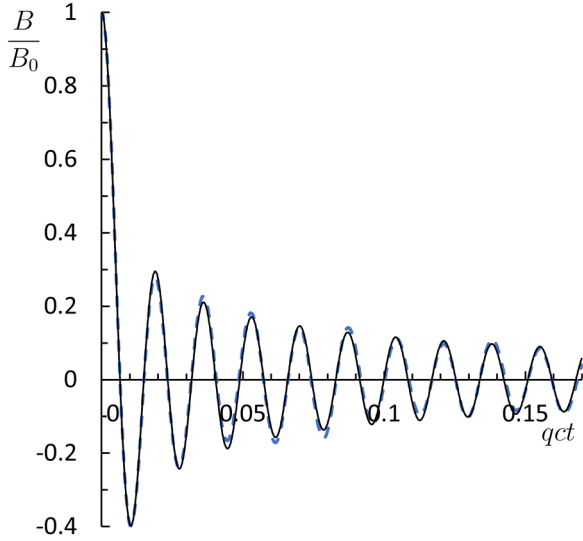
FIG. 5. Time dependence of the amplitude of the sinusoidal temperature profile for $q/\lambda = 2.7 \times 10^{-3}, N = 10^4, N_r = 4.8 \times 10^3$. Analytical solution (68) (black solid line) and simulation results (blue dashed line) are shown.

transition is described by the analytical solution (68). At small times, the analytical solution has a high accuracy, while at large times, the accuracy is lower (see Fig. 7). Determining possible reasons for this discrepancy requires a separate study.

VII. EXAMPLE: UNIFORM TEMPERATURE PROFILE WITH NONZERO FLUX

In this section, we minimize the number of parameters that affect the heat transfer and consider the initial conditions such that the temperature profile is spatially uniform, while the heat flux is not equal to zero. In a purely ballistic regime, which
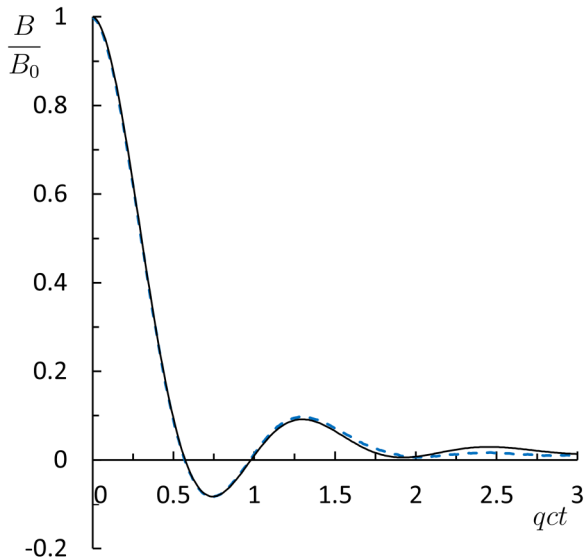

FIG. 6. Time dependence of the amplitude of the sinusoidal temperature profile for $q/\lambda = 0.18, N = 10^4, N_r = 4 \times 10^3$. Analytical solution (68) (black solid line) and simulation results (blue dashed line) are shown.
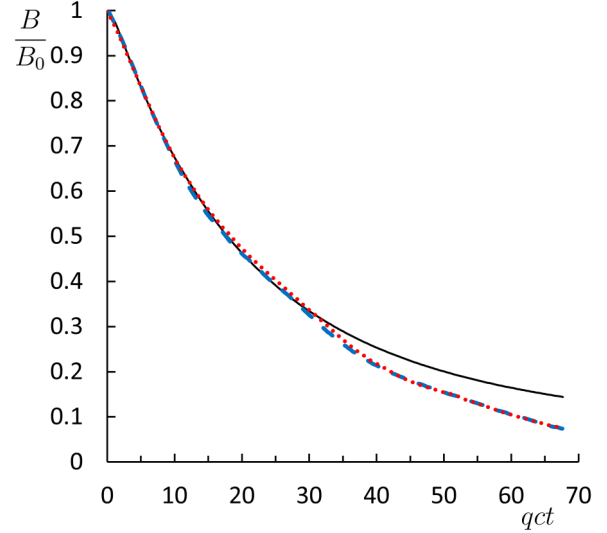

FIG. 7. Time dependence of the amplitude of the sinusoidal temperature profile for $q/\lambda = 2.7$, $N = 5 \times 10^4$, $N_r = 1.4 \times 10^3$. Analytical solution (68) (black solid line) and simulation results for $B_0/T_b = 0.05$ (blue dashed line) and 0.025 (red dots) are shown.

is realized, e.g., in the Hooke chain, the total heat flux is a conserved quantity [27]. Bond dissociation (barriers) leads to decay of the flux due to reflection of the quasiparticles. Therefore in the chain with breaks, the physical mechanism of flux decay is the same as the mechanism, underlying the transition from the ballistic to the diffusive regime of heat transfer. Below we analyze the decay analytically and numerically at different densities of breaks.

We note that the considered statement of the problem differs significantly from the Green-Kubo formalism [38,39]. In the Green-Kubo formalism, the autocorrelation function for the flux at equilibrium is investigated, while in this section we consider the behavior of the flux itself in unsteady nonequilibrium conditions.

A. Analytical solution

In the kinetic model, the following initial conditions are used to specify a uniform temperature profile and a uniform nonzero heat flux:

$$f(0, x, v) = \gamma_1(T_b \phi_1(v) + \Delta T \phi_2(v)),$$

$$\dot{f}(0, x, v) = \gamma_1 \Delta T q|v|(\phi_2(-v) - \phi_2(v)),$$

$$\phi_1(v) = \phi_1(-v), \quad \phi_2(v) = \begin{cases} \phi_+(|v|), & v > 0, \\ \phi_-(|v|), & v < 0, \end{cases}$$

$$\int_{-\infty}^{\infty} \phi_i(v)dv = 1, \quad i = 1, 2, \quad \int_{-\infty}^{\infty} v\phi_2(v)dv \neq 0. \quad (73)$$

Here, the function ϕ_1 sets the velocity distribution of quasiparticles corresponding to the background temperature T_b with zero flux [since function $\phi_1(v)$ is even]. The finite initial heat flux [the last of the conditions (73)] is created by a suitable choice of functions ϕ_+, ϕ_-, which determine the number of quasiparticles with positive and negative velocities. In particular, we further consider the case when all quasiparticles, creating a flux, initially have positive velocities ($\phi_- \equiv 0$,

$\phi_+ \neq 0$). Formulation of the corresponding initial conditions for the equations of motion (1) is discussed in the next subsection.

To obtain the solution of the kinetic equation (26) with the initial conditions (73), we use the fact that the initial conditions are independent from the spatial coordinate. Then the distribution function has the form $f(t, v)$ and Eq. (26) is simplified:

$$\ddot{f} + 2q|v|\dot{f} = 0. \qquad (74)$$

Solving this equation with the initial conditions (73), we obtain

$$f(t, v) = \gamma_1 T_0 \phi_1(v) + \frac{\gamma_1 \Delta T}{2}(\phi_2(v) + \phi_2(-v) \\ + [\phi_2(v) - \phi_2(-v)]e^{-2q|v|t}). \qquad (75)$$

The corresponding temperature and heat flux, calculated by formulas (20), have the forms

$$h(t) = \gamma_2 \Delta T \int_0^\infty (\phi_+(v) - \phi_-(v))e^{-2qvt} v \, dv,$$
$$T(t) = T_b + \Delta T. \qquad (76)$$

This formula shows that in the presence of breaks ($q \neq 0$), the flux decays in time, while the temperature remains constant.

We consider a special case when all quasiparticles initially have positive velocities

$$\phi_- \equiv 0, \quad \phi_+ \neq 0, \quad \int_0^\infty \phi_+(v)dv = 1. \qquad (77)$$

Then using the substitution

$$v = c_g(\kappa), \quad d\kappa = -\tfrac{1}{2}\phi_+(v)dv, \quad \phi_+(v) = -2\big(c_g^{-1}(v)\big)', \qquad (78)$$

we rewrite formula (76) as

$$h(t) = 2\gamma_2 \Delta T \int_0^{1/2} c_g(\kappa)e^{-2qc_g(\kappa)t}d\kappa. \qquad (79)$$

If the group velocity is given by formula (4), the flux (79) is expressed in terms of special functions:

$$h(t) = 2\gamma_2 c\Delta T \int_0^{1/2} e^{-2qct\cos\pi\kappa}\cos\pi\kappa \, d\kappa$$
$$= \gamma_2 c\Delta T (L_{-1}(2qct) - I_1(2qct)), \qquad (80)$$

where $L_{-1}(x)$ is the modified Struve function and $I_1(x)$ is the modified Bessel function.

An analysis of formula (80) shows that the heat flux h decreases monotonically with time from the initial value to zero. The dimensionless flux depends on a single argument—the dimensionless time qct. Consequently, the decay of the flux at different densities of breaks differs only by a time scale.

B. Numerical modeling

To specify a uniform temperature profile and a finite flux in numerical simulations, the approach described in papers [14,40] is used. The particles are given initial velocities and displacements corresponding to a superposition of harmonic

waves traveling in one direction and having random phases.[6] In addition, to create a thermal background, all particles are given random velocities corresponding to a uniform spatial distribution of temperature. As a result, the initial velocities and displacements of particles are set using the formulas

$$u_n = \sum_{j=1}^{N/2-1} A_j \sin\left(\frac{2\pi jn}{N} + \chi_j\right),$$

$$v_n = \varrho_n\sqrt{\frac{2k_B T_b}{m}} - \sum_{j=1}^{N/2-1} A_j \omega_j \cos\left(\frac{2\pi jn}{N} + \chi_j\right),$$

$$\omega_j = 2\sqrt{\frac{C}{m}}\sin\frac{\pi j}{N}, \quad A_j^2 = \frac{4k_B \Delta T}{(N-2)m\omega_j^2},$$

$$\langle\chi_j\rangle = 0, \quad \langle\chi_j\chi_k\rangle = \frac{\pi^2}{3}\delta_{jk}, \quad \langle\chi_j\varrho_n\rangle = 0, \qquad (81)$$

where T_b is the background temperature, ΔT is a part of temperature, corresponding to a finite flux, ϱ_n are random numbers [see formula (5)], and χ_j are random phase shifts (uncorrelated random numbers uniformly distributed in the interval $[-\pi; \pi)$). Here, the wave amplitudes A_j are chosen in such a way as to ensure a uniform distribution of energy among wave numbers.[7]

Under initial conditions (81), the initial kinetic temperatures of all particles are equal, and the energy flux at each point is the same. In the absence of bond dissociation, the energy flux is conserved [27]. The dissociation leads to reflection of waves and decay of the flux. To demonstrate this fact, in simulations the average value of the total energy flux is calculated by formula

$$H(t) = \frac{a}{2}\sum_{n=1}^N \langle F_n(v_n + v_{n-1})\rangle_r. \qquad (82)$$

Due to the spatial homogeneity of the problem, the ratio of the total energy flux to its initial value $H(t)/H_0$ coincides with the analogous ratio for the local heat flux $h(t)/h_0$. The latter is calculated below using formula (80).

In the analytical solution (80), the dimensionless flux $h(t)/h_0$ depends only on the dimensionless time qct. Simulation results can additionally depend on parameters qa, $\Delta T/T_b$, N, and N_r. Further, we consider the influence of the density of breaks q, while other parameters are chosen such that

$$N_r = 2.8 \times 10^3, \quad N = 5 \times 10^4, \quad \frac{\Delta T}{T_b} = 0.05. \qquad (83)$$

Decay of the flux is shown in Fig. 8. It is seen that the characteristic time of the decay is of the order of the time of ballistic-diffusive transition (57). Note that, as in the previous example, in numerical simulations the flux decays faster than

---

[6]Here it is assumed that the chain contains an even number of particles N.

[7]Here we use the fact that the average energy per particle in a wave with an amplitude of A_j and a frequency of ω_j is equal to $\frac{1}{2}mA_j^2\omega_j^2$. Therefore, a uniform distribution of energy among wavenumbers is achieved at $A_j \sim 1/\omega_j$.
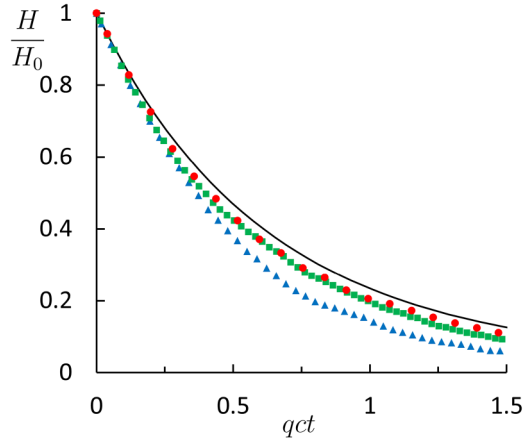
FIG. 8. Decay of the heat flux in a chain with uniform temperature profile and finite initial flux. Analytical solution (80) (solid line) and simulation results for $qa = 1.78 \times 10^{-4}$ (triangles), 4×10^{-6} (squares), and 1.6×10^{-6} (circles) are shown.

predicted by the analytical solution (80). At the same time, as the density of breaks decreases, the difference between the analytical and numerical solutions also decreases.

VIII. ON RELATION BETWEEN LATTICE DYNAMICS AND KINETIC THEORY

In this section, we consider the relation between descriptions of heat transfer in the framework of lattice dynamics and kinetic theory. In particular, we discuss the relation between the velocity distribution of quasiparticles $\phi(v)$ and the group velocity $c_g(\kappa)$. The reasoning is carried out for one-dimensional harmonic crystals with a fairly general dispersion relation.

In Sec. IV B, it is shown that in the ballistic limit (at $q = 0$) evolution of the initial temperature profile $T_0(x)$ is described by the formula

$$T(t, x) = \int_{-\infty}^{\infty} T_0(x - vt)\phi(v)dv. \qquad (84)$$

In papers [11,28], a similar formula is obtained using lattice dynamics:

$$T(t, x) = \int_{0}^{1} T_0(x - c_g(\kappa)t)d\kappa. \qquad (85)$$

Formula (85) is valid for harmonic crystals with a simple structure and interaction of an arbitrary number of neighbors [28]. We show that formulas (84) and (85) can be derived from each other.

We use the following representation of the initial temperature:

$$T_0(x) = \int_{-\infty}^{\infty} \delta(\xi) T_0(x - \xi)d\xi. \qquad (86)$$

Here, the initial temperature profile is divided into a set of point disturbances expressed by delta functions. Substituting the representation (86) into the formula (85) after simple transformations gives

$$T(t, x) = \int_{-\infty}^{\infty} \int_{0}^{1} \delta(\xi - c_g(\kappa)t)T_0(x - \xi)d\kappa \, d\xi. \qquad (87)$$

In this expression, each delta function can be associated with a quasiparticle moving at the group velocity $c_g(\kappa)$. Using this analogy, we consider the following substitution of variables in formula (85)

$$v = c_g(\kappa), \quad \kappa = c_g^{-1}(v), \quad d\kappa = \left(c_g^{-1}(v)\right)' dv. \qquad (88)$$

Here $c_g^{-1}(v)$ is the inverse function with respect to $c_g(\kappa)$. Only the dependencies $c_g(\kappa)$ that monotonically decrease over the interval $\kappa \in [0, 1]$ are considered [see, e.g., (91)]. Using the substitution (88) in formula (85), we get[8]

$$T(t, x) = \int_{-c}^{c} T_0(x - vt)\left(-c_g^{-1}(v)\right)' dv. \qquad (89)$$

It can be seen that this formula coincides with the solution of the kinetic equation (84) if we choose the function $\phi(v)$ such that

$$\phi(v) = -\left(c_g^{-1}(v)\right)' \theta(c^2 - v^2). \qquad (90)$$

Formula (90) determines the relation between the dependence of the group velocity on the wavenumber and the velocity distribution of quasiparticles, provided that quasiparticles with different velocities carry the same amount of energy.

For example, we give explicit formulas for the functions c_g, c_g^{-1}, and ϕ in the case of the Hooke chain:

$$c_g(\kappa) = c \cos(\pi\kappa), \quad c_g^{-1}(v) = \frac{1}{\pi} \arccos\left(\frac{v}{c}\right),$$

$$\phi(v) = \frac{\theta(c^2 - v^2)}{\pi\sqrt{c^2 - v^2}}, \qquad (91)$$

where $\arccos(\cdots)$ is the principal value of the arccosine function.

Thus, formulas (84) and (85) are equivalent up to the substitution of variables (88) and (90). In other words, heat transfer in a one-dimensional harmonic crystal is described by the same equations as motion of an ideal gas of quasiparticles. Formulas (88) and (90) yield the relation between the velocity distribution of quasiparticles $\phi(v)$ and the group velocity $c_g(\kappa)$.

IX. CONCLUSIONS

A kinetic description of heat transfer in the chain with breaks was presented. The heat transfer was modeled by the motion of quasiparticles in a channel with randomly appearing barriers, mimicking dissociated bonds and leading to reflection of quasiparticles. The kinetic equation (26), describing the evolution of the distribution function for quasiarticles, was obtained and solved analytically. Using the distribution function, the fundamental solution for temperature was obtained. Analysis of the fundamental solution has shown that the presence of bond dissociation leads to a transition from the ballistic regime, which is realized at small times ($qct \ll 1$), to the diffusive regime at large times.

To analyze the fundamental solution for temperature, we have introduced the transfer function and the shape function.

---

[8]Here the minus sign before $c_g^{-1}(v)$ occurs due to the fact that when variables are replaced, the integration limits are reversed.

The transfer function characterizes the time dependence of the distance traveled by heat, while the shape function characterizes the spatial distribution of temperature. These functions allow one, in particular, to distinguish between ballistic, diffusive, and anomalous regimes of heat transfer. It has been shown that the transport function in the chain with breaks at large times is proportional to the square root of time, which corresponds to the diffusive regime of heat transfer. At the same time, the shape function differs significantly from the Gaussian function, corresponding to the Fourier law. In particular, the shape function for the chain with breaks has a discontinuity of the first derivative ("a tip") at zero, while the Gaussian function has zero derivative at this point. Therefore, the diffusive regime of heat transfer in the considered system is not described by the Fourier law.

We note that the effective thermal conductivity of the chain with breaks, calculated using the solution of the unsteady problem, in the diffusive regime does not depend on length. This fact is consistent with the results obtained in nonequilibrium steady-state formulation in papers [17,18] for several potentials allowing for bond dissociation. Additionally, we have shown that the length dependence of the thermal conductivity is determined by the transfer function and it is independent of the shape function. Therefore the independence of the effective thermal conductivity on length, generally speaking, does not guarantee the fulfillment of the Fourier law. This fact should be taken into account when interpreting the results of numerical simulations and real experiments on heat transfer.

The question arises as to how to modify the considered chain in order to fulfill the Fourier law. Our solutions of kinetic equations show that if wave propagation in a medium occurs at a single speed (no dispersion), then the Fourier law is satisfied (in the diffusive limit). Hence, classical thermal conductivity can be realized in a hypothetical crystal with bond dissociation, but without dispersion (or with weak dispersion). To create such a model, one can, for example, choose the interactions in the crystal with further neighbors in such a way as to minimize the dispersion. However, testing this hypothesis is beyond the scope of the present paper. Another possibility for achieving Fourier thermal conductivity is to create a system in which the probability of reflection from dissociated bonds is proportional to the squared velocity of quasiparticles in formula (24) it is a linear function of velocity. In this case, the coefficient in the right-hand side of Eq. (52) does not depend on the velocity, and classical diffusion is realized. However, the mechanism that may cause the quadratic dependence of the probability of reflection on the velocity of quasiparticles is not clear yet.

Note that in the chain with breaks (as well as in all other lattices), the initial temperature profile and the initial heat flux can be set independently. In particular, we have presented the initial conditions corresponding to the spatially uniform temperature profile with nonzero heat flux. These initial conditions make it possible, in particular, to exclude the influence of nonuniform distribution of the density of breaks along the chain on the heat transfer. An analytical solution describing decay of the heat flux caused by bond dissociation was obtained. The solution shows that the decay at different densities of breaks differs only in

timescaling, i.e., the flux depends only on the dimensionless time qct.

In conclusion, we note that the presented kinetic model does not reproduce the simulation results exactly. Some differences between the model and simulation results have been demonstrated at large times (see Fig. 7). Our results also suggest that the accuracy of the kinetic model increases with the decreasing density of breaks. However, further investigations of the reasons for these discrepancies are required.

APPENDIX: DISTRIBUTION FUNCTION FOR BOND STRAINS

In this Appendix, we derive formula (9) for the distribution function for strains

$$\varepsilon_n = \frac{u_n - u_{n-1}}{a}. \tag{A1}$$

Using the equations of motion (1), we show that the strains satisfy the equation

$$\dot{v}_n = f_{n+1} - 2f_n + f_{n-1}, \quad \dot{\varepsilon}_n = v_n, \tag{A2}$$

where

$$f_n = f(\varepsilon_n) = \frac{F_n}{ma} = \frac{C\varepsilon_n}{m}\theta(\varepsilon_* - \varepsilon_n). \tag{A3}$$

We consider the probability density function $\Omega(\varepsilon_1, .., \varepsilon_N, v_1, .., v_N, t)$, determining the probability of observing the chain in the vicinity of the point $(\varepsilon_1, .., \varepsilon_N, v_1, .., v_N)$ in the phase space. The probability density function is related to the strain distribution function $\zeta(\varepsilon_i)$ as

$$\zeta(\varepsilon_i) = \int_p \int_{s \neq i} \Omega \, d\varepsilon_s dv_p$$

$$= \int_{-\infty}^{+\infty} \cdots \int_{-\infty}^{+\infty} \Omega \, d\varepsilon_1 ... d\varepsilon_{i-1} d\varepsilon_{i+1} ... d\varepsilon_N dv_1 ... dv_N. \tag{A4}$$

According to the Liouville's theorem, Ω satisfies the balance equation:

$$\frac{\partial \Omega}{\partial t} + \sum_{n=1}^{N} \left(\frac{\partial \Omega}{\partial \varepsilon_n} v_n + \frac{\partial \Omega}{\partial v_n} \dot{v}_n \right) = 0. \tag{A5}$$

To find $\zeta(\varepsilon_i)$, we consider a stationary case of Eq. (A5) and integrate it with respect to all ε_s, $s \neq i$ and all v_p, $p \neq i$, using identities

$$(\Omega v_s)\big|_{\varepsilon_s \to -\infty}^{\varepsilon_s \to +\infty} \to 0, \quad (\Omega \dot{v}_p)\big|_{v_p \to -\infty}^{v_p \to +\infty} \to 0. \tag{A6}$$

Here $\Omega \to 0$ at infinity due to the normalization condition. Then (A5) takes the form

$$\frac{\partial \Omega_i}{\partial \varepsilon_i} v_i + \frac{\partial}{\partial v_i} \int_{-\infty}^{+\infty} \int_{-\infty}^{+\infty} \Omega_i^* \dot{v}_i \, d\varepsilon_{i-1} d\varepsilon_{i+1} = 0,$$

$$\Omega_i^*(\varepsilon_i, v_i, \varepsilon_{i-1}, \varepsilon_{i+1}) = \int_{p \neq i} \int_{s < i-1, s > i+1} \Omega \, d\varepsilon_s dv_p,$$

$$\Omega_i(\varepsilon_i, v_i) = \int_{-\infty}^{+\infty} \int_{-\infty}^{+\infty} \Omega_i^* d\varepsilon_{i-1} d\varepsilon_{i+1}. \tag{A7}$$

We assume that strains and velocities of at least three neighboring bonds are independent and seek for a solution of (A7) in the form

$$\Omega_i^* = \zeta(\varepsilon_i)\eta(v_i)\zeta(\varepsilon_{i-1})\zeta(\varepsilon_{i+1}), \tag{A8}$$

where functions ζ, η satisfy the normalization conditions

$$\int_{-\infty}^{+\infty} \zeta(\varepsilon_i) d\varepsilon_i = \int_{-\infty}^{+\infty} \eta(v_i) dv_i = 1. \tag{A9}$$

Substituting formula (A8) into Eq. (A7), we obtain

$$\zeta'(\varepsilon)\eta(v)v + 2\zeta(\varepsilon)\eta'(v)(\bar{f} - f(\varepsilon)) = 0,$$

$$\bar{f} = \int_{-\infty}^{+\infty} \zeta(\varepsilon) f(\varepsilon) d\varepsilon. \tag{A10}$$

Here index i is omitted for brevity. Since ε and v are independent, then Eq. (A10) is equivalent to the system of equations

$$\frac{\eta(v)}{\eta'(v)} v = A, \qquad \frac{2\zeta(\varepsilon)}{\zeta'(\varepsilon)}(f(\varepsilon) - \bar{f}) = A. \tag{A11}$$

From the first equation in (A11) and normalization condition (A9) it follows that η is the Gaussian distribution

$$\eta(v) = \frac{e^{-v^2/(2\sigma^2)}}{\sqrt{2\pi\sigma^2}}, \qquad \sigma^2 = \langle v^2 \rangle = \frac{2k_B T}{ma^2}. \tag{A12}$$

Then the second equation from (A11) has the solution

$$\zeta = \zeta_0 \exp\left[\frac{ma^2}{k_B T}\left(\bar{f}\varepsilon - \int_0^\varepsilon f(\varepsilon) d\varepsilon\right)\right], \tag{A13}$$

where ζ_0 is determined by the normalization condition. Substituting $\bar{f} = -p_T/(ma)$ and formula (A3) into (A13), we obtain formula (9). A similar result was obtained by different means in papers [41,42].

---

[1] G. Chen, Non-Fourier phonon heat conduction at the microscale and nanoscale, Nat. Rev. Phys. **3**, 555 (2021).

[2] R. Kovács, Heat equations beyond Fourier: From heat waves to thermal metamaterials, Phys. Rep. **1048**, 1 (2024).

[3] D. G. Cahill, W. K. Ford, K. E. Goodson, G. D. Mahan, A. Majumdar, H. J. Maris, R. Merlin, and S. R. Phillpot, Nanoscale thermal transport, J. Appl. Phys. **93**, 793 (2003).

[4] C. W. Chang, D. Okawa, H. Garcia, A. Majumdar, and A. Zettl, Breakdown of Fouriers law in nanotube thermal conductors, Phys. Rev. Lett. **101**, 075903 (2008).

[5] M. E. Pumarol, M. C. Rosamond, P. Tovee, M. C. Petty, D. A. Zeze, V. Falko, and O. V. Kolosov, Direct nanoscale imaging of ballistic and diffusive thermal transport in graphene nanostructures, Nano Lett. **12**, 2906 (2012).

[6] R. Anufriev, Y. Wu, S. Volz, and M. Nomura, Quasi-ballistic thermal transport in silicon carbide nanowires, Appl. Phys. Lett. **124**, 022202 (2024).

[7] S. Lepri, R. Livi, and A. Politi, Thermal conduction in classical low-dimensional lattices, Phys. Rep. **377**, 1 (2003).

[8] *Thermal Transport in Low Dimensions: From Statistical Physics to Nanoscale Heat Transfer*, edited by S. Lepri (Springer, New York, 2016), Vol. 921.

[9] G. Benenti, S. Lepri, and R. Livi, Anomalous heat transport in classical many-body systems: Overview and perspectives, Front. Phys. **8**, 292 (2020).

[10] Z. Rieder, J. L. Lebowitz, and E. Lieb, Properties of a harmonic crystal in a stationary nonequilibrium state, J. Math. Phys. **8**, 1073 (1967).

[11] A. M. Krivtsov, Heat transfer in infinite harmonic one-dimensional crystals, Dokl. Phys. **60**, 407 (2015).

[12] A. M. Krivtsov, The ballistic heat equation for a one-dimensional harmonic crystal, in *Dynamical Processes in Generalized Continua and Structures*, edited by H. Altenbach, A. Belyaev, V. A. Eremeyev, A. Krivtsov, and A. V. Porubov (Springer, Berlin, 2019).

[13] V. A. Kuzkin and A. M. Krivtsov, Ballistic resonance and thermalization in Fermi-Pasta-Ulam-Tsingou chain at finite temperature, Phys. Rev. E **101**, 042209 (2020).

[14] E. A. Korznikova, V. A. Kuzkin, A. M. Krivtsov, D. Xiong, V. A. Gani, A. A. Kudreyko, and S. V. Dmitriev, Equilibration of sinusoidal modulation of temperature in linear and nonlinear chains, Phys. Rev. E **102**, 062148 (2020).

[15] S. D. Liazhkov and V. A. Kuzkin, Unsteady two-temperature heat transport in mass-in-mass chains, Phys. Rev. E **105**, 054145 (2022).

[16] G. Dematteis, L. Rondoni, D. Proment, F. De Vita, and M. Onorato, Coexistence of ballistic and Fourier regimes in the β Fermi-Pasta-Ulam-Tsingou lattice, Phys. Rev. Lett. **125**, 024101 (2020).

[17] O. V. Gendelman and A. V. Savin, Normal heat conductivity in chains capable of dissociation, Europhys. Lett. **106**, 34004 (2014).

[18] A. V. Savin and Y. A. Kosevich, Thermal conductivity of molecular chains with asymmetric potentials of pair interactions, Phys. Rev. E **89**, 032102 (2014).

[19] R. Peierls, Zur kinetischen theorie der warmeleitung in kristallen, Ann. Phys. **395**, 1055 (1929).

[20] H. Spohn, The phonon Boltzmann equation, properties and link to weakly anharmonic lattice dynamics, J. Stat. Phys. **124**, 1041 (2006).

[21] V. A. Kuzkin and A. M. Krivtsov, Unsteady ballistic heat transport: Linking lattice dynamics and kinetic theory, Acta Mech. **232**, 1983 (2021).

[22] J. Lukkarinen, Kinetic theory of phonons in weakly anharmonic particle chains, in *Thermal Transport in Low Dimensions*, Lecture Notes in Physics Vol. 921 (Springer, Cham, 2016).

[23] A. Mellet and S. Merino-Aceituno, Anomalous energy transport in FPU-β chain, J. Stat. Phys. **160**, 583 (2015).

[24] S. Denisov, J. Klafter, and M. Urbakh, Dynamical heat channels, Phys. Rev. Lett. **91**, 194301 (2003).

[25] P. Cipriani, S. Denisov, and A. Politi, From anomalous energy diffusion to Levy walks and heat conductivity in one-dimensional systems, Phys. Rev. Lett. **94**, 244301 (2005).

[26] A. Dhar, K. Saito, and B. Derrida, Exact solution of a Levy walk model for anomalous heat transport, Phys. Rev. E **87**, 010103(R) (2013).

[27] A. M. Krivtsov, Dynamics of matter and energy, Z. Angew. Math. Mech. **103**, e202100496 (2023).

[28] V. A. Kuzkin and A. M. Krivtsov, Fast and slow thermal processes in harmonic scalar lattices, J. Phys.: Condens. Matter **29**, 505401 (2017).

[29] A. M. Krivtsov, From nonlinear oscillations to equation of state in simple discrete systems, Chaos, Solitons Fractals **17**, 79 (2003).

[30] A. M. Krivtsov and V. A. Kuzkin, Derivation of equations of state for ideal crystals of simple structure, Mech. Solids **46**, 387 (2011).

[31] V. A. Kuzkin and A. M. Krivtsov, Nonlinear positive/negative thermal expansion and equations of state of a chain with longitudinal and transverse vibrations, Phys. Status Solidi B **252**, 1664 (2015).

[32] T. Rubin, H. W. Altman, and H. L. Johnston, Coefficients of thermal expansion of solids at low temperatures. I. The thermal expansion of copper from 15 to 300 K, J. Am. Chem. Soc. **76**, 5289 (1954).

[33] A. D. Polyanin, *Handbook of Linear Partial Differential Equations for Engineers and Scientists* (Chapman and Hall, London/CRC, 2016).

[34] A. Dhar, A. Kundu, and A. Kundu, Anomalous heat transport in one dimensional systems: A description using non-local fractional-type diffusion equation, Front. Phys. **7**, 159 (2019).

[35] J. A. Johnson, A. A. Maznev, J. Cuffe, J. K. Eliason, A. J. Minnich, T. Kehoe, Clivia M. Sotomayor Torres, G. Chen, and K. A. Nelson, Direct measurement of room-temperature nondiffusive thermal transport over micron distances in a silicon membrane, Phys. Rev. Lett. **110**, 025901 (2013).

[36] J. A. Rogers, A. A. Maznev, M. J. Banet, and K. A. Nelson, Optical generation and characterization of acousticwaves in thin films: Fundamentals and applications, Annu. Rev. Mater. Sci. **30**, 117 (2000).

[37] S. Huberman, R. A. Duncan, K. Chen, B. Song, V. Chiloyan, Z. Ding, A. A. Maznev, G. Chen, and K. A. Nelson, Observation of second sound in graphite at temperatures above 100 K, Science **364**, 375 (2019).

[38] M. Green, Markoff random processes and the statistical mechanics of time-dependent phenomena. II. Irreversible processes in fluids, J. Chem. Phys. **22**, 398 (1954).

[39] R. Kubo, Statistical-mechanical theory of irreversible processes. I. General theory and simple applications to magnetic and conduction problems, J. Phys. Soc. Jpn. **12**, 570 (1957).

[40] S. V. Dmitriev, V. A. Kuzkin, and A. M. Krivtsov, Nonequilibrium thermal rectification at the junction of harmonic chains, Phys. Rev. E **108**, 054221 (2023).

[41] J. S. Dugdale and D. K. C. MacDonald, Vibrational anharmonicity and lattice thermal properties, Phys. Rev. **96**, 57 (1954).

[42] F. Gürsey and H. Jones, *Classical Statistical Mechanics of a Rectilinear Assembly* (Imperial College of Science and Technology, London, 1948).